

Berry Curvature Spectroscopy from Bloch Oscillations

Christophe De Beule^{1,2} and E. J. Mele¹

¹*Department of Physics and Astronomy, University of Pennsylvania, Philadelphia PA 19104*

²*Department of Physics and Materials Science, University of Luxembourg, L-1511 Luxembourg, Luxembourg*

(Dated: May 25, 2023)

We demonstrate that the Berry curvature of an isolated Bloch miniband in two-dimensional superlattices can be probed by the *dressed* linear optical response when a uniform static field is applied to the system. In particular, when the static field is sufficiently strong such that full Bloch oscillations occur before the crystal momentum relaxes to equilibrium, the optical response of the dressed system becomes resonant at the Bloch frequencies. The latter are in the THz regime when the superlattice periodicity is of the order of 10 nm. Using a band-projected semiclassical theory, we define a dressed optical conductivity and find that the height of the resonances in the dressed *Hall* conductivity are proportional to the Fourier components of the Berry curvature. We illustrate our results with a low-energy model on an effective honeycomb lattice.

Nonlinear optical responses are becoming an increasingly important tool to investigate the spectral and geometric properties of electron Bloch bands in low-dimensional materials [1–3]. In particular, the nonlinear Hall effect [4] which probes the multipoles of the Berry curvature of the band at successive orders in the driving field [5]. The distribution of the Berry curvature can be studied by nonlinear response even in crystals with time-reversal symmetry, which show no linear Hall effect, since time-reversal symmetry only precludes odd powers of the field in the Hall response. Recently, the advent of moiré [6–8] and other two-dimensional (2D) superlattice materials [9–11] has opened up the prospect of studying responses at nonperturbative order in the driving field [12–14]. These systems can host spectrally isolated and flattened minibands, and nonlinear responses have already been used to study their properties [15–22]. Moreover, because the real-space periodicity of such superlattices can be much larger than the underlying atomic scale, with lattice constants ranging between 1–100 nm, the momentum space superlattice Brillouin zone (BZ) is relatively small. Under an applied electric field, it therefore becomes possible that an electron traverses the *entire* zone, i.e., performs a full Bloch oscillation [23, 24], before relaxing back to equilibrium by scattering processes. To quantify this, consider an applied uniform electric field of the form

$$\mathbf{E}(t) = \mathbf{E}_0 + \mathbf{E}_1(t), \quad (1)$$

which has a static component $\mathbf{E}_0 = E_0(\cos\theta_0, \sin\theta_0)$ and an oscillating component $\mathbf{E}_1(t)$. The latter acts as a weak probe for the system that is *dressed* by the static field. Here, the nonperturbative regime is defined by the condition $\omega_B\tau \gg 1$ [12–14] where $\omega_B = eE_0L/\hbar$ is the characteristic frequency of Bloch oscillations, which we call the Bloch frequency, and τ is the momentum-relaxation time with L the lattice constant. If we estimate $\tau = 1$ ps we find that $\omega_B\tau \approx \frac{1.5E_0}{\text{kV/cm}} \frac{L}{10 \text{ nm}}$ such that $\omega_B\tau$ can become large in superlattice materials for reasonable field strengths [12, 13].

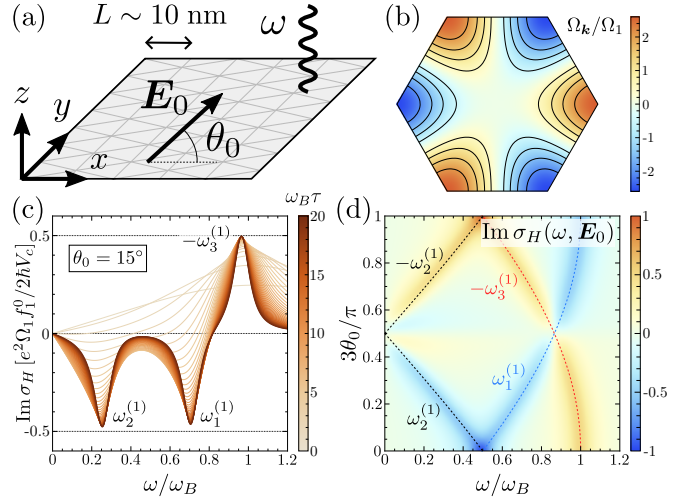


FIG. 1. (a) 2D superlattice (e.g., a moiré) subjected to a static uniform in-plane electric field \mathbf{E}_0 and probed by monochromatic light of frequency ω . (b) Berry curvature $\Omega_{\mathbf{k}}/\Omega_1$ in the first-shell approximation for a system with D_3 or C_{3v} symmetry. (c) Imaginary part of the dressed optical Hall conductivity $\sigma_H(\omega, \mathbf{E}_0)$ for the Berry curvature shown in (b) as a function of ω/ω_B for $\theta_0 = 15^\circ$ and different values of $\omega_B\tau$. (d) $\text{Im} \sigma_H$ in units $e^2\Omega_1 f_1^0/2\hbar V_c$ for $\omega_B\tau = 15$ as a function of the frequency and the field direction θ_0 . The resonant frequencies for the first shell $\omega_n^{(1)} = |e\mathbf{E}_0 \cdot \mathbf{L}_n/\hbar|$ are indicated.

In this work, we study the dressed time-dependent response of time-reversal-invariant 2D superlattices with lattice constants $L \sim 10$ nm, that are subjected to a uniform electric field of the form given in Eq. (1). This setup is illustrated in Fig. 1(a). When the static field is in the nonperturbative regime, we find an optical response, linear in the *oscillating* component, that is resonant at the Bloch frequencies. For the studied systems, the latter are on the order of 10 THz. Moreover, we show that the peak heights of the resonances in the dressed optical *Hall* conductivity are proportional to the Fourier components of the Berry curvature. Hence our approach is in some sense dual to probing the momentum-space distribution of the

Berry curvature via its multipoles at successive harmonics [25] and complementary to other methods that study orbital moments with circular dichroism [26]. In contrast, in our proposal, all information on the Berry curvature is contained in the dressed *linear* optical response.

Semiclassical theory. Our starting point is the band-projected semiclassical theory of electron dynamics for a 2D crystal in a uniform electric field $\mathbf{E}(t)$. The equations of motion for the central position and crystal momentum of a wave packet constructed from the Bloch states of an energy band $\varepsilon_{n\mathbf{k}}$ are given by [27, 28]

$$\hbar\dot{\mathbf{r}}_{n\mathbf{k}} = \nabla_{\mathbf{k}}\varepsilon_{n\mathbf{k}} - \hbar\dot{\mathbf{k}} \times \Omega_{n\mathbf{k}}\hat{z}, \quad (2)$$

$$\hbar\dot{\mathbf{k}} = -e\mathbf{E}(t), \quad (3)$$

where $-e$ is the electron charge and $\Omega_{n\mathbf{k}} = -2\text{Im}\langle\partial_{k_x}u_{n\mathbf{k}}|\partial_{k_y}u_{n\mathbf{k}}\rangle_{\text{cell}}$ is the Berry curvature [29]. The band-projected theory holds as long as interband transitions can be neglected. These can arise both from optical transitions and electric breakdown (Zener tunneling) [30]. The former are absent for frequencies well below the energy gap to the other energy bands ε_{gap} , while the absence of the latter can be estimated by the condition that $\varepsilon_{\text{gap}}^2/\varepsilon_{\text{width}} \gg eE_0L$ where $\varepsilon_{\text{width}}$ is the bandwidth [13, 14].

In the following, we drop the band index n since we consider a single band. The current is then given by

$$\mathbf{j}(t) = -e \int_{\mathbf{k}} \dot{\mathbf{r}}_{\mathbf{k}}(t) f_{\mathbf{k}}(t), \quad (4)$$

with $\int_{\mathbf{k}} = \int_{\text{BZ}} d^2\mathbf{k}/(2\pi)^2$ and where $f_{\mathbf{k}}(t)$ is the nonequilibrium occupation of the electrons in the band. The latter is obtained from the Boltzmann transport equation in the relaxation-time approximation:

$$\tau\partial_t f_{\mathbf{k}} - \frac{e\tau}{\hbar}\mathbf{E}(t) \cdot \nabla_{\mathbf{k}} f_{\mathbf{k}} = f_{\mathbf{k}}^0 - f_{\mathbf{k}}, \quad (5)$$

where τ is the momentum-relaxation time and $f_{\mathbf{k}}^0 = n_F(\varepsilon_{\mathbf{k}} - \mu)$ with n_F the Fermi function and μ the chemical potential. Because the system has translational symmetry, the occupation function is periodic in momentum space: $f_{\mathbf{k}} = \sum_{\mathbf{R}} f_{\mathbf{R}} e^{i\mathbf{k}\cdot\mathbf{R}}$ where the sum runs over lattice vectors \mathbf{R} with $f_{\mathbf{R}} = V_c \int_{\mathbf{k}} f_{\mathbf{k}} e^{-i\mathbf{k}\cdot\mathbf{R}}$. Plugging this expansion in Eq. (S5) we obtain an ordinary differential equation with the steady-state solution [31]

$$f_{\mathbf{R}}(t) = f_{\mathbf{R}}^0 \int_0^\infty ds e^{-s} \exp\left[\frac{ie}{\hbar} \int_{t-s\tau}^t dt' \mathbf{E}(t') \cdot \mathbf{R}\right], \quad (6)$$

as shown in the Supplemental Material (SM) [32]. The occupation $f_{\mathbf{k}}$ is thus given by a weighted sum of displaced Fermi functions where the drift due to the electric field is determined by the accumulated momentum between collisions at time $t-s\tau$ and time t . The exponential weight e^{-s} reflects the fact that scattering is modeled as a Poisson process in the relaxation-time approximation.

The current in Eq. (4) can be decomposed into two terms as $\mathbf{j}(t) = \mathbf{j}_{\text{Bloch}}(t) + \mathbf{j}_{\text{geom}}(t)$ where

$$\mathbf{j}_{\text{Bloch}}(t) = \frac{ie}{\hbar V_c} \sum_{\mathbf{R}} \mathbf{R} \varepsilon_{-\mathbf{R}} f_{\mathbf{R}}(t), \quad (7)$$

$$\mathbf{j}_{\text{geom}}(t) = \hat{z} \times \frac{e^2}{\hbar V_c} \sum_{\mathbf{R}} \Omega_{-\mathbf{R}} \mathbf{E}(t) f_{\mathbf{R}}(t), \quad (8)$$

where V_c is the unit cell area and we made use of the expansions of the band dispersion and the Berry curvature, as well as $V_c \int_{\mathbf{k}} e^{i\mathbf{k}\cdot\mathbf{R}} = \delta_{\mathbf{R},\mathbf{0}}$. The Bloch current $\mathbf{j}_{\text{Bloch}}$ originates from the band dispersion while the geometric current \mathbf{j}_{geom} originates from the anomalous velocity due to the Berry curvature in Eq. (2).

Dressed optical conductivity. We now consider probing the system by monochromatic light of frequency ω at normal incidence. In the electric-dipole approximation, the electric field of the light can be written as

$$\mathbf{E}_1(t) = \mathcal{E}_1 e^{i\omega t} + \mathcal{E}_1^* e^{-i\omega t}, \quad (9)$$

where $\mathcal{E}_1 \in \mathbb{C}^2$ gives the polarization. To investigate the response of the system at frequency ω , we expand the lattice Fourier components of the distribution function in terms of their frequency components. We have $f_{\mathbf{R}}(t) = \sum_{m=-\infty}^{\infty} f_{\mathbf{R},m} e^{im\omega t}$ where $f_{\mathbf{R},m} = (\omega/2\pi) \int_0^{2\pi/\omega} dt f_{\mathbf{R}}(t) e^{-im\omega t}$ with $f_{\mathbf{R},-m} = f_{-\mathbf{R},m}^*$. The frequency components of the currents become

$$\mathbf{j}_{\text{Bloch}}^{(m)} = \frac{ie}{\hbar V_c} \sum_{\mathbf{R}} \mathbf{R} \varepsilon_{-\mathbf{R}} f_{\mathbf{R},m}, \quad (10)$$

$$\mathbf{j}_{\text{geom}}^{(m)} = \hat{z} \times \frac{e^2}{\hbar V_c} \sum_{\mathbf{R}} \Omega_{-\mathbf{R}} \cdot (\mathbf{E}_0 f_{\mathbf{R},m} + \mathcal{E}_1 f_{\mathbf{R},m-1} + \mathcal{E}_1^* f_{\mathbf{R},m+1}). \quad (11)$$

Since we are interested in the linear response *dressed* by the static part of the field, we expand Eq. (6) in orders of $|e\mathcal{E}_1 \cdot \mathbf{R}/\hbar\omega|$ while retaining all orders in \mathbf{E}_0 . Up to first order, the only nonzero terms are given by

$$f_{\mathbf{R},0} = \frac{f_{\mathbf{R}}^0}{1 - i\omega_{\mathbf{R}}\tau}, \quad (12)$$

$$f_{\mathbf{R},1} = \frac{f_{\mathbf{R}}^0}{1 - i\omega_{\mathbf{R}}\tau} \frac{e\mathcal{E}_1 \cdot \mathbf{R}/\hbar}{\omega - \omega_{\mathbf{R}} - \frac{i}{\tau}} = f_{-\mathbf{R},-1}^*, \quad (13)$$

with $\omega_{\mathbf{R}} = e\mathbf{E}_0 \cdot \mathbf{R}/\hbar$. The response at frequency ω can then be written as $j_a^{(1)} = \sigma_{ab} \mathcal{E}_{1b}$ where $a, b = x, y$ and summation over repeated indices is implied. This leads us to the main result of this work: the *dressed* optical conductivity

$$\sigma_{ab}(\omega, \mathbf{E}_0) = \frac{ie^2}{\hbar^2 V_c} \sum_{\mathbf{R}} \frac{R_a R_b \varepsilon_{-\mathbf{R}} f_{\mathbf{R}}^0}{(1 - i\omega_{\mathbf{R}}\tau) (\omega - \omega_{\mathbf{R}} - \frac{i}{\tau})} - \frac{e^2}{\hbar V_c} \sum_{\mathbf{R}} \frac{\Omega_{-\mathbf{R}} f_{\mathbf{R}}^0}{1 - i\omega_{\mathbf{R}}\tau} \left[\epsilon_{ab} + \frac{e\epsilon_{ac} E_{0c} R_b/\hbar}{\omega - \omega_{\mathbf{R}} - \frac{i}{\tau}} \right], \quad (14)$$

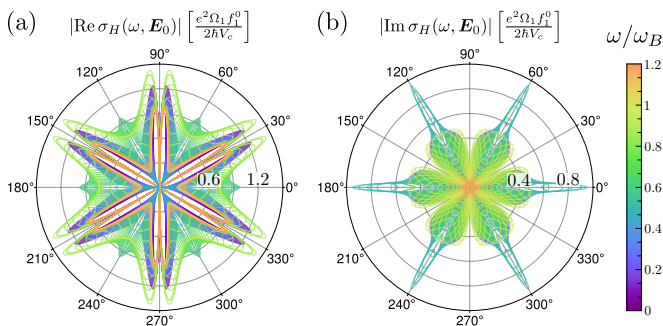


FIG. 2. Roses for the real (a) and imaginary (b) part of the dressed optical Hall conductivity $\sigma_H(\omega, \mathbf{E}_0)$ for the Berry curvature shown in Fig. 1(b) with $\omega_B\tau = 15$. The angle corresponds to the direction of the static electric field θ_0 and the color scale gives the frequency ω of the oscillating field.

where ϵ_{ab} is the permutation symbol and $\sigma_{ab}(\omega, \mathbf{E}_0)^* = \sigma_{ab}(-\omega, \mathbf{E}_0)$ such that the real (imaginary) part is even (odd) in ω . As a check, we undress the conductivity by setting $E_0 = 0$. In this case, the two terms in Eq. (14) reduce to the Drude and anomalous Hall conductivity, respectively. Importantly, the dressed linear Hall response does *not* vanish when time-reversal symmetry is conserved, because it is effectively a compound nonlinear response in the fields \mathbf{E}_0 and $\mathbf{E}_1(t)$.

Let us now focus on the case where \mathbf{E}_0 is finite and consider the dressed longitudinal $\sigma_L = \delta_{ab}\sigma_{ab}/2$ and Hall $\sigma_H = \epsilon_{ab}\sigma_{ab}/2$ conductivities, which transform as a scalar and pseudoscalar under coordinate transformations, respectively. We obtain

$$\sigma_L = \frac{ie^2}{2\hbar^2 V_c} \sum_{\mathbf{R}} \frac{R^2 \epsilon_{-\mathbf{R}} f_{\mathbf{R}}^0}{(1 - i\omega_B\tau)(\omega - \omega_{\mathbf{R}} - \frac{i}{\tau})}, \quad (15)$$

$$\sigma_H = -\frac{e^2}{\hbar V_c} \sum_{\mathbf{R}} \frac{\Omega_{-\mathbf{R}} f_{\mathbf{R}}^0}{1 - i\omega_B\tau} \left(1 + \frac{1}{2} \frac{\omega_{\mathbf{R}}}{\omega - \omega_{\mathbf{R}} - \frac{i}{\tau}} \right), \quad (16)$$

which for $\omega_B\tau \gg 1$ simplify to

$$\sigma_L(\omega, \mathbf{E}_0) = -\frac{e^2}{\hbar} \frac{\pi}{\tau V_c} \sum_{\mathbf{R}} \frac{R^2 \epsilon_{-\mathbf{R}} f_{\mathbf{R}}^0}{\hbar \omega_{\mathbf{R}} (\omega - \omega_{\mathbf{R}} - \frac{i}{\tau})}, \quad (17)$$

$$\sigma_H(\omega, \mathbf{E}_0) = -\frac{e^2}{\hbar} \frac{\pi}{\tau V_c} \sum_{\mathbf{R}} \frac{i\Omega_{-\mathbf{R}} f_{\mathbf{R}}^0}{\omega - \omega_{\mathbf{R}} - \frac{i}{\tau}}. \quad (18)$$

For crystals with time-reversal symmetry, the band dispersion (Berry curvature) is an even (odd) function of momentum, such that $\epsilon_{\mathbf{R}}$ and $f_{\mathbf{R}}^0$ are real, while $\Omega_{\mathbf{R}}$ is imaginary. In this case, $\text{Im}\sigma_L$ and $\text{Im}\sigma_H$ are given by a series of Lorentzians centered at the Bloch frequencies $\omega_{\mathbf{R}}$ in the nonperturbative limit. The height of these resonances is proportional to $\epsilon_{\mathbf{R}}$ and $\Omega_{\mathbf{R}}$, respectively, and independent of the relaxation time τ . Conversely, the real part of the dressed conductivity vanishes at resonance. Physically, we can interpret this as the transfer of energy from the incident light into coherent Bloch motion of the electrons. And since we assume here that

$\omega_B\tau \gg 1$, the system is essentially collisionless on the time scale set by the Bloch oscillations.

These results can thus potentially be used to map out the distribution of the Berry curvature in systems with time-reversal symmetry by measuring the resonances in the dressed optical Hall conductivity in the nonperturbative regime where $\omega_B\tau \gg 1$.

First-shell approximation. It is instructive to first evaluate the dressed optical conductivity by only taking into account the leading-order terms in the sum over the lattice vectors. For concreteness, we consider a system with point group D_3 or C_{3v} which lacks inversion or C_{2z} rotation symmetry. In this case, the Berry curvature is generally nonzero even though the Chern number of the band vanishes. In the first-shell approximation, we only take into account the shortest nonzero lattice vectors such that $\epsilon_{\mathbf{k}} = \epsilon_1 \sum_{n=1}^3 \cos(\mathbf{k} \cdot \mathbf{L}_n)$ up to an overall constant and $\Omega_{\mathbf{k}} = \Omega_1 \sum_{n=1}^3 \sin(\mathbf{k} \cdot \mathbf{L}_n)$ where ϵ_1 and Ω_1 are real parameters that depend on the details of the system, and $\mathbf{L}_1 = L(1/2, \sqrt{3}/2)$, $\mathbf{L}_2 = (-L, 0)$, and $\mathbf{L}_3 = -(\mathbf{L}_1 + \mathbf{L}_2)$ are related by C_{3z} rotation symmetry [13, 14].

The imaginary part of the dressed optical Hall conductivity is shown in Fig. 1(c) as a function of ω for $\theta_0 = 15^\circ$ and different values of $\omega_B\tau$. There are three resonances in this case because the first coordination shell supports three Bloch frequencies $\omega_n^{(1)} = |e\mathbf{E}_0 \cdot \mathbf{L}_n|$ which are non-degenerate for a general field direction. The height of these resonances is approximately equal due to C_{3z} and time-reversal symmetry and saturates to $e^2\Omega_1 f_1^0 / 2\hbar V_c$ in the limit $\omega_B\tau \gg 1$, where $f_1^0 = f_{\mathbf{R}=\mathbf{L}_n}^0$. Notice that the resonances are only well-defined for $\omega_B\tau \gtrsim 10$. The dependence on the direction of the static field is shown in Fig. 1(c). Here we show $\text{Im}\sigma_H$ for $\omega_B\tau = 15$ as a function of ω and θ_0 . As we rotate the static field, the resonances move along the curves $\omega = \pm\omega_B \cos(\theta_0 - \theta_n)$ with $\theta_n = \{\pi/3, \pi, -\pi/3\}$. For the special case $\theta_0 = m\pi/3$ ($m \in \mathbb{Z}$) two Bloch frequencies coincide and the peaks are doubled. On the contrary, for $\theta_0 = (2m+1)\pi/6$ the response vanishes due to \mathcal{M}_x ($x \mapsto -x$) mirror symmetry. These features can also be seen in the rose plots of Fig. 2. Here we clearly see that the strongest resonance occurs when two lattice vectors have the same projection along the static field. Away from these directions, the resonance splits into two peaks that shift to higher and lower frequencies.

Low-energy model. Going beyond the first-shell approximation, we now consider a low-energy model defined on an effective honeycomb lattice with one orbital per site, and with nearest-neighbor hopping amplitude $t > 0$ and a sublattice-staggering potential m . The Bloch Hamiltonian is given by

$$\mathcal{H}(\mathbf{k}) = \mathbf{d}(\mathbf{k}) \cdot \boldsymbol{\sigma}, \quad (19)$$

$$\mathbf{d}(\mathbf{k}) = (-t \text{Re } g_{\mathbf{k}}, -t \text{Im } g_{\mathbf{k}}, m), \quad (20)$$

where $\boldsymbol{\sigma} = (\sigma_x, \sigma_y, \sigma_z)$ are the Pauli matrices and $g_{\mathbf{k}} =$

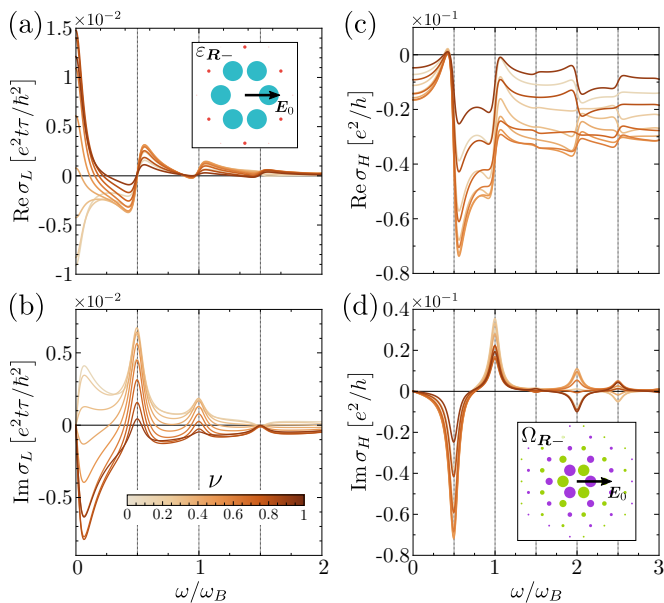


FIG. 3. Dressed optical conductivities $\sigma_L(\omega, \mathbf{E}_0)$ and $\sigma_H(\omega, \mathbf{E}_0)$ for the valence band of the effective two-band model with $m/t = 0.5$ where $\omega_B \tau = 15$, $\theta_0 = 0^\circ$, and $k_B T/t = 0.004$. The color scale gives the filling ν [see inset of (b)]. (a, b) Real and imaginary part of the longitudinal conductivity. (c, d) Real and imaginary part of the Hall conductivity. Dashed vertical lines give the position of the resonances ω_R and the inset in (a) and (d) shows the relative magnitude and phase of ε_{R-} and Ω_{R-} , respectively.

$e^{-i\mathbf{k}\cdot\boldsymbol{\tau}} [1 + e^{i\mathbf{k}\cdot\mathbf{L}_1} + e^{i\mathbf{k}\cdot(\mathbf{L}_1+\mathbf{L}_2)}]$ with $\boldsymbol{\tau} = L\hat{y}/\sqrt{3}$ the relative separation of the two sublattices. Note that we work in periodic gauge for which the semiclassical equation given in Eq. (2) is valid [28, 33]. This model has time-reversal symmetry with point group C_{3v} generated by C_{3z} and \mathcal{M}_x , and can be seen as a minimal low-energy model for moirés such as hBN-aligned twisted bilayer graphene [34, 35] or twisted double bilayer graphene [36, 37], as well as other superlattice systems belonging to the same symmetry class such as periodically-buckled graphene with a C_{3v} height profile [14, 38–40].

The model gives two energy bands $\varepsilon_{\mathbf{k}\pm} = \pm|\mathbf{d}(\mathbf{k})|$ that are separated by a gap $|2m|$ at the zone corners. Because C_{2z} symmetry is broken by the sublattice potential, the Berry curvature is nonzero and given by

$$\Omega_{\mathbf{k}\pm} = \pm \frac{mt^2 V_c}{6|\mathbf{d}(\mathbf{k})|^3} \sum_{n=1}^3 \sin(\mathbf{k} \cdot \mathbf{L}_n), \quad (21)$$

with $V_c = \sqrt{3}L^2/2$. In the limit $|m/t| \gg 1$, we have $|\mathbf{d}(\mathbf{k})| \simeq |m|$ and the first shell dominates with $\Omega_1 = \pm \text{sgn}(m)V_c t^2/6m^2$. However, in general many shells contribute, as illustrated in Fig. 3 where we show $\sigma_L(\omega, \mathbf{E}_0)$ in panels (a) and (b), and $\sigma_H(\omega, \mathbf{E}_0)$ in panels (c) and (d) for $m/t = 0.5$ and different fillings ν of the valence band. Here the static field lies along the x direction and $k_B T/t \ll 1$. Note σ_L decays faster with fre-

quency than σ_H because the first shell of the dispersion is dominant [see inset of Fig. 3(a)] as well as the additional factor of $1/\omega$ in Eq. (17). Note that the filling ν enters only through the Fourier components of the Fermi function f_R^0 which modulate the height of the peaks in the imaginary part of the conductivities and can change sign as a function of ν , see Fig. 3(d).

In conclusion, we developed a band-projected semiclassical theory for the optical response of a superlattice material that is dressed by a uniform static field. When the static field is sufficiently strong, which is achieved for field strengths of the order of 10 kV/cm for a lattice constant of order 10 nm, the dressed system becomes resonant at the frequencies of Bloch oscillations which are in the 10 THz regime. We quantified this effect by defining a dressed optical conductivity whose imaginary part displays peaks at the Bloch frequencies, while the real part vanishes at resonance. In particular, the height of the resonances in the optical Hall conductivity probes the Berry curvature distribution of the electronic band. The dressed optical conductivity can for example be obtained from THz Faraday rotation and ellipticity spectroscopy measurements [41, 42]. Our work thus provides a novel route to probe the Berry curvature in superlattice materials with time-reversal symmetry.

We thank V. T. Phong for discussions. This research was funded in whole, or in part, by the Luxembourg National Research Fund (FNR) (project No. 16515716). CDB and EJM are supported by the Department of Energy under grant DE-FG02-84ER45118.

-
- [1] T. Morimoto and N. Nagaosa, Topological nature of nonlinear optical effects in solids, *Science Advances* **2**, e1501524 (2016).
 - [2] L. Wu, S. Patankar, T. Morimoto, N. L. Nair, E. Thewalt, A. Little, J. G. Analytis, J. E. Moore, and J. Orenstein, Giant anisotropic nonlinear optical response in transition metal mononitride weyl semimetals, *Nature Physics* **13**, 350 (2017).
 - [3] J. Ahn, G.-Y. Guo, N. Nagaosa, and A. Vishwanath, Riemannian geometry of resonant optical responses, *Nature Physics* **18**, 290 (2022).
 - [4] I. Sodemann and L. Fu, Quantum Nonlinear Hall Effect Induced by Berry Curvature Dipole in Time-Reversal Invariant Materials, *Phys. Rev. Lett.* **115**, 216806 (2015).
 - [5] C.-P. Zhang, X.-J. Gao, Y.-M. Xie, H. C. Po, and K. T. Law, Higher-order nonlinear anomalous Hall effects induced by Berry curvature multipoles, *Phys. Rev. B* **107**, 115142 (2023).
 - [6] E. Y. Andrei and A. H. MacDonald, Graphene bilayers with a twist, *Nature Materials* **19**, 1265 (2020).
 - [7] E. Y. Andrei, D. K. Efetov, P. Jarillo-Herrero, A. H. MacDonald, K. F. Mak, T. Senthil, E. Tutuc, A. Yazdani, and A. F. Young, The marvels of moiré materials, *Nat. Rev. Mater.* **6**, 201 (2021).
 - [8] K. F. Mak and J. Shan, Semiconductor moiré materials,

Nature Nanotechnology **17**, 686 (2022).

- [9] R. R., *Superlattice to Nanoelectronics* (Elsevier Science, 2005).
- [10] C. Forsythe, X. Zhou, K. Watanabe, T. Taniguchi, A. Papaty, P. Moon, M. Koshino, P. Kim, and C. R. Dean, Band structure engineering of 2D materials using patterned dielectric superlattices, *Nat. Nanotechnol.* **13**, 566 (2018).
- [11] J. Mao, S. P. Milovanović, M. Andelković, X. Lai, Y. Cao, K. Watanabe, T. Taniguchi, L. Covaci, F. M. Peeters, A. K. Geim, Y. Jiang, and E. Y. Andrei, Evidence of flat bands and correlated states in buckled graphene superlattices, *Nature* **584**, 215 (2020).
- [12] A. Fahimniya, Z. Dong, E. I. Kiselev, and L. Levitov, Synchronizing Bloch-Oscillating Free Carriers in Moiré Flat Bands, *Phys. Rev. Lett.* **126**, 256803 (2021).
- [13] V. T. Phong and E. J. Mele, Quantum Geometric Oscillations in Two-Dimensional Flat-Band Solids (2022), [arXiv:2212.12852 \[cond-mat.mes-hall\]](https://arxiv.org/abs/2212.12852).
- [14] C. D. Beule, V. T. Phong, and E. J. Mele, Rose patterns in the nonperturbative current response of two-dimensional superlattices (2023), [arXiv:2305.03013 \[cond-mat.mes-hall\]](https://arxiv.org/abs/2305.03013).
- [15] P. A. Pantaleón, T. Low, and F. Guinea, Tunable large Berry dipole in strained twisted bilayer graphene, *Phys. Rev. B* **103**, 205403 (2021).
- [16] Z. He and H. Weng, Giant nonlinear Hall effect in twisted bilayer WTe₂, *npj Quantum Materials* **6**, 101 (2021).
- [17] S. Sinha, P. C. Adak, A. Chakraborty, K. Das, K. Deb Nath, L. D. V. Sangani, K. Watanabe, T. Taniguchi, U. V. Waghmare, A. Agarwal, and M. M. Deshmukh, Berry curvature dipole senses topological transition in a moiré superlattice, *Nature Physics* **18**, 765 (2022).
- [18] A. Chakraborty, K. Das, S. Sinha, P. C. Adak, M. M. Deshmukh, and A. Agarwal, Nonlinear anomalous Hall effects probe topological phase-transitions in twisted double bilayer graphene, *2D Materials* **9**, 045020 (2022).
- [19] C.-P. Zhang, J. Xiao, B. T. Zhou, J.-X. Hu, Y.-M. Xie, B. Yan, and K. T. Law, Giant nonlinear Hall effect in strained twisted bilayer graphene, *Phys. Rev. B* **106**, L041111 (2022).
- [20] P. A. Pantaleón, V. o. T. Phong, G. G. Naumis, and F. Guinea, Interaction-enhanced topological Hall effects in strained twisted bilayer graphene, *Phys. Rev. B* **106**, L161101 (2022).
- [21] J. Duan, Y. Jian, Y. Gao, H. Peng, J. Zhong, Q. Feng, J. Mao, and Y. Yao, Giant Second-Order Nonlinear Hall Effect in Twisted Bilayer Graphene, *Phys. Rev. Lett.* **129**, 186801 (2022).
- [22] J. Zhong, J. Duan, S. Zhang, H. Peng, Q. Feng, Y. Hu, Q. Wang, J. Mao, J. Liu, and Y. Yao, Effective manipulation and realization of a colossal nonlinear Hall effect in an electric-field tunable moiré system (2023), [arXiv:2301.12117 \[cond-mat.mes-hall\]](https://arxiv.org/abs/2301.12117).
- [23] F. Bloch, Über die Quantenmechanik der Elektronen in Kristallgittern, *Zeitschrift für Physik* **52**, 555 (1929).
- [24] K. Leo, P. H. Bolivar, F. Brüggemann, R. Schwedler, and K. Köhler, Observation of Bloch oscillations in a semiconductor superlattice, *Solid State Communications* **84**, 943 (1992).
- [25] T. T. Luu and H. J. Wörner, Measurement of the Berry curvature of solids using high-harmonic spectroscopy, *Nature Communications* **9**, 916 (2018).
- [26] M. Schüler, U. D. Giovannini, H. Hübener, A. Rubio, M. A. Sentef, and P. Werner, Local Berry curvature signatures in dichroic angle-resolved photoelectron spectroscopy from two-dimensional materials, *Science Advances* **6**, eaay2730 (2020).
- [27] M.-C. Chang and Q. Niu, Berry Phase, Hyperorbits, and the Hofstadter Spectrum, *Phys. Rev. Lett.* **75**, 1348 (1995).
- [28] G. Sundaram and Q. Niu, Wave-packet dynamics in slowly perturbed crystals: Gradient corrections and Berry-phase effects, *Phys. Rev. B* **59**, 14915 (1999).
- [29] To construct a wave packet $|W(t)\rangle = \int_{\mathbf{k}} c_{\mathbf{k}}(t) |\Psi_{\mathbf{k}}\rangle$, the Bloch states $|\Psi_{\mathbf{k}}\rangle = e^{i\mathbf{k}\cdot\hat{\mathbf{r}}} |u_{\mathbf{k}}\rangle$ should be smooth on the BZ torus, i.e., $|\Psi_{\mathbf{k}+\mathbf{G}}\rangle = |\Psi_{\mathbf{k}}\rangle$ with \mathbf{G} a reciprocal lattice vector. This is periodic gauge [33] and yields $|u_{\mathbf{k}+\mathbf{G}}\rangle = e^{-i\mathbf{G}\cdot\hat{\mathbf{r}}} |u_{\mathbf{k}}\rangle$, in contrast to $|\tilde{u}_{\mathbf{k}+\mathbf{G}}\rangle = |\tilde{u}_{\mathbf{k}}\rangle$ for which the Bloch Hamiltonian is periodic (Bloch form). The Berry curvature is generally different in both gauges.
- [30] N. W. Ashcroft and N. D. Mermin, *Solid State Physics* (Saunders College Publishing, 1976).
- [31] S. A. Mikhailov, Nonperturbative quasiclassical theory of the nonlinear electrodynamic response of graphene, *Phys. Rev. B* **95**, 085432 (2017).
- [32] See Supplemental Material at [link] for a detailed calculation of the occupation function and the dressed optical conductivity.
- [33] D. Vanderbilt, *Berry Phases in Electronic Structure Theory* (Cambridge University Press, 2018).
- [34] Y.-H. Zhang, D. Mao, and T. Senthil, Twisted bilayer graphene aligned with hexagonal boron nitride: Anomalous Hall effect and a lattice model, *Phys. Rev. Res.* **1**, 033126 (2019).
- [35] C. Lewandowski and L. Levitov, Intrinsically undamped plasmon modes in narrow electron bands, *Proceedings of the National Academy of Sciences* **116**, 20869 (2019).
- [36] M. Koshino, Band structure and topological properties of twisted double bilayer graphene, *Phys. Rev. B* **99**, 235406 (2019).
- [37] N. R. Chebrolov, B. L. Chittari, and J. Jung, Flat bands in twisted double bilayer graphene, *Phys. Rev. B* **99**, 235417 (2019).
- [38] S. P. Milovanović, M. Andelković, L. Covaci, and F. M. Peeters, Band flattening in buckled monolayer graphene, *Phys. Rev. B* **102**, 245427 (2020).
- [39] V. T. Phong and E. J. Mele, Boundary Modes from Periodic Magnetic and Pseudomagnetic Fields in Graphene, *Phys. Rev. Lett.* **128**, 176406 (2022).
- [40] Q. Gao, J. Dong, P. Ledwith, D. Parker, and E. Khalaf, Untwisting moiré physics: Almost ideal bands and fractional Chern insulators in periodically strained monolayer graphene (2022), [arXiv:2211.00658 \[cond-mat.mes-hall\]](https://arxiv.org/abs/2211.00658).
- [41] S. Spielman, B. Parks, J. Orenstein, D. T. Nemetz, F. Ludwig, J. Clarke, P. Merchant, and D. J. Lew, Observation of the Quasiparticle Hall Effect in Superconducting YBa₂Cu₃O_{7- δ} , *Phys. Rev. Lett.* **73**, 1537 (1994).
- [42] R. Shimano, Y. Ikebe, K. S. Takahashi, M. Kawasaki, N. Nagaosa, and Y. Tokura, Terahertz Faraday rotation induced by an anomalous Hall effect in the itinerant ferromagnet SrRuO₃, *Europhysics Letters* **95**, 17002 (2011).

Supplemental Material for ‘‘Berry Curvature Spectroscopy from Bloch Oscillations’’

SEMICLASSICAL MODEL OF ELECTRON DYNAMICS

The semiclassical equations of motion for an electron in a two-dimensional (2D) crystal, occupying an energy band with dispersion $\varepsilon_{n\mathbf{k}}$ subjected to a uniform electric field $\mathbf{E}(t)$ are given by [27, 28]

$$\hbar\dot{\mathbf{r}}_{n\mathbf{k}} = \nabla_{\mathbf{k}}\varepsilon_{n\mathbf{k}} - \hbar\dot{\mathbf{k}} \times \boldsymbol{\Omega}_{n\mathbf{k}}, \quad (\text{S1a})$$

$$\hbar\dot{\mathbf{k}} = -e\mathbf{E}(t), \quad (\text{S1b})$$

where the dot stands for the time derivative d/dt . Here $e > 0$ is the elementary charge, n is the band index, and $\boldsymbol{\Omega}_{n\mathbf{k}} = \Omega_{n\mathbf{k}}\hat{z}$ is the Berry curvature. The latter is defined as

$$\Omega_{n\mathbf{k}} = i \left(\left\langle \frac{\partial u_{n\mathbf{k}}}{\partial k_x} \middle| \frac{\partial u_{n\mathbf{k}}}{\partial k_y} \right\rangle_{\text{cell}} - \left\langle \frac{\partial u_{n\mathbf{k}}}{\partial k_y} \middle| \frac{\partial u_{n\mathbf{k}}}{\partial k_x} \right\rangle_{\text{cell}} \right), \quad (\text{S2})$$

where $u_{n\mathbf{k}}(\mathbf{r})$ are cell-periodic Bloch functions in periodic gauge, $u_{n,\mathbf{k}+\mathbf{G}}(\mathbf{r}) = e^{-i\mathbf{G}\cdot\mathbf{r}}u_{n\mathbf{k}}(\mathbf{r})$ with \mathbf{G} a reciprocal lattice vector, and $\langle u_{n\mathbf{k}} | u_{m\mathbf{k}} \rangle_{\text{cell}} = \delta_{nm}$.

In the following, we consider a single band and omit the band index n . The band dispersion and Berry curvature can be expanded as

$$\varepsilon_{\mathbf{k}} = \sum_{\mathbf{R}} \varepsilon_{\mathbf{R}} e^{i\mathbf{k}\cdot\mathbf{R}}, \quad \Omega_{\mathbf{k}} = \sum_{\mathbf{R}} \Omega_{\mathbf{R}} e^{i\mathbf{k}\cdot\mathbf{R}}, \quad (\text{S3})$$

where

$$\varepsilon_{\mathbf{R}} = V_c \int_{\mathbf{k}} \varepsilon_{\mathbf{k}} e^{-i\mathbf{k}\cdot\mathbf{R}}, \quad \Omega_{\mathbf{R}} = V_c \int_{\mathbf{k}} \Omega_{\mathbf{k}} e^{-i\mathbf{k}\cdot\mathbf{R}}, \quad \int_{\mathbf{k}} = \int_{\text{BZ}} \frac{d^2\mathbf{k}}{(2\pi)^2}. \quad (\text{S4})$$

BOLTZMANN TRANSPORT EQUATION

The Boltzmann equation for the distribution function $f(\mathbf{k}, \mathbf{r}, t)$ in the relaxation-time approximation, is given by

$$\frac{\partial f}{\partial t} + \frac{d\mathbf{k}}{dt} \cdot \nabla_{\mathbf{k}} f + \frac{d\mathbf{r}}{dt} \cdot \nabla_{\mathbf{r}} f = \frac{f^0 - f}{\tau}, \quad (\text{S5})$$

where $f^0(\mathbf{k})$ is the equilibrium distribution function, i.e., $f^0(\mathbf{k}) = n_F(\varepsilon_{\mathbf{k}} - \mu)$ with $n_F(z) = 1/(e^{z/k_B T} + 1)$ the Fermi function, with μ the chemical potential and T the temperature.

Let us consider a general uniform time-dependent electric field $\mathbf{E}(t)$. We are interested in the steady-state solutions (not necessarily static) of

$$\frac{\partial f}{\partial t} - \frac{e}{\hbar} \mathbf{E}(t) \cdot \nabla_{\mathbf{k}} f = \frac{f^0 - f}{\tau}. \quad (\text{S6})$$

In a translational-invariant system,

$$f(\mathbf{k}, t) = \sum_{\mathbf{R}} f_{\mathbf{R}}(t) e^{i\mathbf{k}\cdot\mathbf{R}}, \quad (\text{S7})$$

where \mathbf{R} are lattice vectors, and similarly for $f^0(\mathbf{k})$. We then obtain an ordinary differential equation for each Fourier component $f_{\mathbf{R}}(t)$,

$$\frac{df_{\mathbf{R}}}{dt} + \left(\frac{1}{\tau} - \frac{ie}{\hbar} \mathbf{E}(t) \cdot \mathbf{R} \right) f_{\mathbf{R}}(t) = \frac{f_{\mathbf{R}}^0}{\tau}, \quad (\text{S8})$$

whose general solution is given by

$$f_{\mathbf{R}}(t) = \frac{f_{\mathbf{R}}^0}{\tau} \int_{t_0}^t dt' e^{-\frac{t-t'}{\tau}} \exp \left[\frac{ie}{\hbar} \int_{t'}^t du \mathbf{E}(u) \cdot \mathbf{R} \right], \quad (\text{S9})$$

with t_0 an integration constant. In the static limit, i.e., for a time-independent electric field, we have

$$\lim_{\mathbf{E}(t) \rightarrow \mathbf{E}} f_{\mathbf{R}}(t) = \frac{f_{\mathbf{R}}^0}{\tau} \int_{t_0}^t dt' e^{-(t-t')\left(\frac{1}{\tau} - ie\mathbf{E} \cdot \mathbf{R}/\hbar\right)} = f_{\mathbf{R}}^0 \frac{1 - e^{-\frac{t-t_0}{\tau}(1-ie\tau\mathbf{E} \cdot \mathbf{R}/\hbar)}}{1 - ie\tau\mathbf{E} \cdot \mathbf{R}/\hbar}. \quad (\text{S10})$$

The steady-state solution is thus given by

$$f_{\mathbf{R}}(t) = \frac{f_{\mathbf{R}}^0}{\tau} \int_{-\infty}^t dt' e^{-\frac{t-t'}{\tau}} \exp\left[\frac{ie}{\hbar} \int_{t'}^t du \mathbf{E}(u) \cdot \mathbf{R}\right] \quad (\text{S11})$$

$$= f_{\mathbf{R}}^0 \int_0^{\infty} ds e^{-s} \exp\left[\frac{ie}{\hbar} \int_{t-s\tau}^t dt' \mathbf{E}(t') \cdot \mathbf{R}\right], \quad (\text{S12})$$

where $s = (t - t')/\tau$. The exponential factor can be interpreted as the integrated momentum shift between two scattering events at $t - s\tau$ and t . Going back to momentum space, we have [31]

$$f(\mathbf{k}, t) = \sum_{\mathbf{R}} f_{\mathbf{R}}(t) e^{i\mathbf{k} \cdot \mathbf{R}} = \int_0^{\infty} ds e^{-s} f^0 \left(\mathbf{k} + \frac{e}{\hbar} \int_{t-s\tau}^t dt' \mathbf{E}(t') \cdot \mathbf{R} \right). \quad (\text{S13})$$

We now consider the following driving field:

$$\mathbf{E}(t) = \mathbf{E}_0 + \mathbf{E}_1(t), \quad \mathbf{E}_1(t) = \boldsymbol{\mathcal{E}}_1 e^{i\omega t} + \boldsymbol{\mathcal{E}}_1^* e^{-i\omega t} = 2 \text{Re}(\boldsymbol{\mathcal{E}}_1 e^{i\omega t}), \quad (\text{S14})$$

where $E_0 = |\mathbf{E}_0|$ is large compared to $E_1 = |\mathbf{E}_1|$. In this case, the Fourier components of the distribution function become

$$f_{\mathbf{R}}(t) = f_{\mathbf{R}}^0 \int_0^{\infty} ds e^{-(1 - \frac{ie\tau}{\hbar} \mathbf{E}_0 \cdot \mathbf{R})s} \exp\left[\frac{ie}{\hbar} \int_{t-s\tau}^t dt' \mathbf{E}_1(t') \cdot \mathbf{R}\right] \quad (\text{S15})$$

$$= f_{\mathbf{R}}^0 \int_0^{\infty} ds e^{-(1 - \frac{ie\tau}{\hbar} \mathbf{E}_0 \cdot \mathbf{R})s} \exp\left[\frac{ie}{\hbar} \left(\frac{\boldsymbol{\mathcal{E}}_1 \cdot \mathbf{R}}{i\omega} e^{i\omega t} (1 - e^{-i\omega s\tau}) + \text{c.c.} \right)\right]. \quad (\text{S16})$$

Up to first order in E_1 , we can expand this as

$$f_{\mathbf{R}}(t) \simeq \frac{f_{\mathbf{R}}^0}{1 - ie\tau\mathbf{E}_0 \cdot \mathbf{R}/\hbar} + \frac{ie f_{\mathbf{R}}^0}{\hbar} \int_0^{\infty} ds e^{-(1 - \frac{ie\tau}{\hbar} \mathbf{E}_0 \cdot \mathbf{R})s} \left[\frac{\boldsymbol{\mathcal{E}}_1 \cdot \mathbf{R}}{i\omega} e^{i\omega t} (1 - e^{-i\omega s\tau}) + \text{c.c.} \right] \quad (\text{S17})$$

$$= \frac{f_{\mathbf{R}}^0}{1 - ie\tau\mathbf{E}_0 \cdot \mathbf{R}/\hbar} \left[1 + \frac{e\boldsymbol{\mathcal{E}}_1 \cdot \mathbf{R}/\hbar}{\omega - e\mathbf{E}_0 \cdot \mathbf{R}/\hbar - \frac{i}{\tau}} e^{i\omega t} - \frac{e\boldsymbol{\mathcal{E}}_1^* \cdot \mathbf{R}/\hbar}{\omega + e\mathbf{E}_0 \cdot \mathbf{R}/\hbar + \frac{i}{\tau}} e^{-i\omega t} \right]. \quad (\text{S18})$$

Defining the frequency-space Fourier components as

$$f_{\mathbf{R}}(t) = \sum_{m=-\infty}^{\infty} f_{\mathbf{R},m} e^{im\omega t}, \quad f_{\mathbf{R},m}(\omega) = \frac{\omega}{2\pi} \int_0^{2\pi/\omega} dt f_{\mathbf{R}}(t) e^{-im\omega t}, \quad (\text{S19})$$

with $f_{\mathbf{R},-m} = f_{-\mathbf{R},m}^*$, we have, for example,

$$f_{\mathbf{R},0} = \frac{f_{\mathbf{R}}^0}{1 - ie\tau\mathbf{E}_0 \cdot \mathbf{R}/\hbar} \left[1 - \frac{2|e\boldsymbol{\mathcal{E}}_1 \cdot \mathbf{R}/\hbar|^2}{(\omega - e\mathbf{E}_0 \cdot \mathbf{R}/\hbar - \frac{i}{\tau})(\omega + e\mathbf{E}_0 \cdot \mathbf{R}/\hbar + \frac{i}{\tau})} + \mathcal{O}(E_1^4) \right], \quad (\text{S20})$$

$$f_{\mathbf{R},1} = \frac{f_{\mathbf{R}}^0}{1 - ie\tau\mathbf{E}_0 \cdot \mathbf{R}/\hbar} \left[\frac{e\boldsymbol{\mathcal{E}}_1 \cdot \mathbf{R}/\hbar}{\omega - e\mathbf{E}_0 \cdot \mathbf{R}/\hbar - \frac{i}{\tau}} + \mathcal{O}(E_1^3) \right], \quad (\text{S21})$$

$$f_{\mathbf{R},2} = \frac{f_{\mathbf{R}}^0}{1 - ie\tau\mathbf{E}_0 \cdot \mathbf{R}/\hbar} \left[\frac{e\boldsymbol{\mathcal{E}}_1 \cdot \mathbf{R}/\hbar}{\omega - e\mathbf{E}_0 \cdot \mathbf{R}/\hbar - \frac{i}{\tau}} \frac{e\boldsymbol{\mathcal{E}}_1 \cdot \mathbf{R}/\hbar}{2\omega - e\mathbf{E}_0 \cdot \mathbf{R}/\hbar - \frac{i}{\tau}} + \mathcal{O}(E_1^4) \right]. \quad (\text{S22})$$

DRESSED OPTICAL CONDUCTIVITY

The steady-state current is given by $\mathbf{j}(t) = \mathbf{j}_{\text{Bloch}}(t) + \mathbf{j}_{\text{geom}}(t)$ with

$$\mathbf{j}_{\text{Bloch}}(t) = -e \int_{\mathbf{k}} f_{\mathbf{k}}(t) \nabla_{\mathbf{k}} \varepsilon_{\mathbf{k}} = \frac{ie}{\hbar V_c} \sum_{\mathbf{R}} \mathbf{R} \varepsilon_{-\mathbf{R}} f_{\mathbf{R}}(t), \quad (\text{S23})$$

$$\mathbf{j}_{\text{geom}}(t) = -\frac{e^2}{\hbar} [\mathbf{E}(t) \times \hat{z}] \int_{\mathbf{k}} f_{\mathbf{k}}(t) \Omega_{\mathbf{k}} = \frac{e^2}{\hbar V_c} \hat{z} \times \sum_{\mathbf{R}} \Omega_{-\mathbf{R}} \mathbf{E}(t) f_{\mathbf{R}}(t), \quad (\text{S24})$$

with

$$V_c \int_{\mathbf{k}} e^{i\mathbf{k} \cdot \mathbf{R}} = \delta_{\mathbf{R}, \mathbf{0}}, \quad \sum_{\mathbf{R}} e^{i\mathbf{k} \cdot \mathbf{R}} = \frac{(2\pi)^2}{V_c} \delta(\mathbf{k}). \quad (\text{S25})$$

The frequency components of the currents are thus given by

$$\mathbf{j}_{\text{Bloch}}^{(m)}(\omega) = \frac{ie}{\hbar V_c} \sum_{\mathbf{R}} \mathbf{R} \varepsilon_{-\mathbf{R}} f_{\mathbf{R}, m}, \quad (\text{S26})$$

$$\mathbf{j}_{\text{geom}}^{(m)}(\omega) = \frac{e^2}{\hbar V_c} \hat{z} \times \sum_{\mathbf{R}} \Omega_{-\mathbf{R}} (\mathbf{E}_0 f_{\mathbf{R}, m} + \mathcal{E}_1 f_{\mathbf{R}, m-1} + \mathcal{E}_1^* f_{\mathbf{R}, m+1}), \quad (\text{S27})$$

with $\mathbf{j}^{(-m)} = (\mathbf{j}^{(m)})^*$. For example, the DC component of the geometric current becomes

$$\mathbf{j}_{\text{geom}}^{(0)}(\omega) = \frac{e^2}{\hbar V_c} \hat{z} \times \sum_{\mathbf{R}} \frac{\Omega_{-\mathbf{R}} f_{\mathbf{R}}^0}{1 - ie\tau \mathbf{E}_0 \cdot \mathbf{R}/\hbar} \left\{ \left[1 - \frac{2|e\mathcal{E}_1 \cdot \mathbf{R}/\hbar|^2}{(\omega - e\mathbf{E}_0 \cdot \mathbf{R}/\hbar - \frac{i}{\tau})(\omega + e\mathbf{E}_0 \cdot \mathbf{R}/\hbar + \frac{i}{\tau})} \right] \mathbf{E}_0 \right. \quad (\text{S28})$$

$$\left. + \left[\frac{(e\mathcal{E}_1 \cdot \mathbf{R}/\hbar) \mathcal{E}_1^*}{\omega - e\mathbf{E}_0 \cdot \mathbf{R}/\hbar - \frac{i}{\tau}} - \frac{(e\mathcal{E}_1^* \cdot \mathbf{R}/\hbar) \mathcal{E}_1}{\omega + e\mathbf{E}_0 \cdot \mathbf{R}/\hbar + \frac{i}{\tau}} \right] + \mathcal{O}(E_1^4) \right\}. \quad (\text{S29})$$

In lowest order of $|e\mathcal{E}_1 \cdot \mathbf{R}/\hbar\omega|$, the first harmonics are given by

$$\mathbf{j}_{\text{Bloch}}^{(1)}(\omega) = \frac{ie}{\hbar V_c} \sum_{\mathbf{R}} \frac{\mathbf{R} \varepsilon_{-\mathbf{R}} f_{\mathbf{R}}^0}{1 - ie\tau \mathbf{E}_0 \cdot \mathbf{R}/\hbar} \frac{e\mathcal{E}_1 \cdot \mathbf{R}/\hbar}{\omega - e\mathbf{E}_0 \cdot \mathbf{R}/\hbar - \frac{i}{\tau}}, \quad (\text{S30})$$

$$\mathbf{j}_{\text{geom}}^{(1)}(\omega) = \frac{e^2}{\hbar V_c} \hat{z} \times \sum_{\mathbf{R}} \frac{\Omega_{-\mathbf{R}} f_{\mathbf{R}}^0}{1 - ie\tau \mathbf{E}_0 \cdot \mathbf{R}/\hbar} \left[\mathcal{E}_1 + \frac{(e\mathcal{E}_1 \cdot \mathbf{R}/\hbar) \mathbf{E}_0}{\omega - e\mathbf{E}_0 \cdot \mathbf{R}/\hbar - \frac{i}{\tau}} \right]. \quad (\text{S31})$$

We now define the *dressed* optical conductivity $\sigma_{ij}(\omega, \mathbf{E}_0)$ through $j_i^{(1)} = \sigma_{ij} \mathcal{E}_{1j}$. The current can thus be written as

$$j_i(t) = j_i^{(0)} + 2 \text{Re} [\sigma_{ij}(\omega, \mathbf{E}_0) \mathcal{E}_{1j} e^{i\omega t}] + \mathcal{O}(E_1^2). \quad (\text{S32})$$

Making use of $(\mathbf{a} \times \mathbf{b})_i = \epsilon_{ijk} a^j b^k$ with $\epsilon_{i3k} = -\epsilon_{ik}$ the permutation symbol, we find

$$\sigma_{ij}(\omega, \mathbf{E}_0) = \frac{ie^2}{\hbar^2 V_c} \sum_{\mathbf{R}} \frac{R_i R_j \varepsilon_{-\mathbf{R}} f_{\mathbf{R}}^0}{(1 - ie\tau \mathbf{E}_0 \cdot \mathbf{R}/\hbar)(\omega - e\mathbf{E}_0 \cdot \mathbf{R}/\hbar - \frac{i}{\tau})} \quad (\text{S33})$$

$$- \frac{\epsilon_{ik} e^2}{\hbar V_c} \sum_{\mathbf{R}} \frac{\Omega_{-\mathbf{R}} f_{\mathbf{R}}^0}{1 - ie\tau \mathbf{E}_0 \cdot \mathbf{R}/\hbar} \left[\delta_{kj} + \frac{eE_{0k} R_j/\hbar}{\omega - e\mathbf{E}_0 \cdot \mathbf{R}/\hbar - \frac{i}{\tau}} \right], \quad (\text{S34})$$

with $\sigma_{ij}(\omega, \mathbf{E}_0) = \sigma_{ij}(-\omega, \mathbf{E}_0)^*$. As a check, we undress the conductivity:

$$\sigma_{ij}(\omega, \mathbf{0}) = \frac{ie^2}{\hbar^2 V_c} \sum_{\mathbf{R}} \frac{R_i R_j \varepsilon_{-\mathbf{R}} f_{\mathbf{R}}^0}{\omega - \frac{i}{\tau}} - \epsilon_{ij} \frac{e^2}{\hbar} \frac{1}{V_c} \sum_{\mathbf{R}} \Omega_{-\mathbf{R}} f_{\mathbf{R}}^0 \quad (\text{S35})$$

$$= \frac{e^2}{\hbar^2} \int_{\mathbf{k}} f_{\mathbf{k}}^0 \frac{\partial_i \partial_j \varepsilon_{\mathbf{k}}}{i\omega + \frac{1}{\tau}} - \epsilon_{ij} \frac{e^2}{\hbar} \int_{\mathbf{k}} f_{\mathbf{k}}^0 \Omega_{\mathbf{k}}, \quad (\text{S36})$$

with $\partial_i = \partial/\partial k_i$. This is a well-known result for the conductivity: the first term is the Drude contribution and the second term is the anomalous Hall conductivity.

Let us now consider the dressed longitudinal conductivity $\sigma_L = (\sigma_{xx} + \sigma_{yy})/2$ which is a scalar and the dressed Hall conductivity, $\sigma_H = (\sigma_{xy} - \sigma_{yx})/2$ which is a pseudoscalar. We find

$$\sigma_L(\omega, \mathbf{E}_0) = \frac{ie^2}{2\hbar^2 V_c} \sum_{\mathbf{R}} \frac{R^2 \varepsilon_{-\mathbf{R}} f_{\mathbf{R}}^0}{(1 - ie\tau \mathbf{E}_0 \cdot \mathbf{R}/\hbar) (\omega - e\mathbf{E}_0 \cdot \mathbf{R}/\hbar - \frac{i}{\tau})}, \quad (\text{S37})$$

$$\sigma_H(\omega, \mathbf{E}_0) = \frac{1}{2} \varepsilon_{ij} \sigma_{ij} = -\frac{e^2}{\hbar} \frac{1}{V_c} \sum_{\mathbf{R}} \frac{\Omega_{-\mathbf{R}} f_{\mathbf{R}}^0}{1 - ie\tau \mathbf{E}_0 \cdot \mathbf{R}/\hbar} \left(1 + \frac{1}{2} \frac{e\mathbf{E}_0 \cdot \mathbf{R}/\hbar}{\omega - e\mathbf{E}_0 \cdot \mathbf{R}/\hbar - \frac{i}{\tau}} \right), \quad (\text{S38})$$

where we used $\varepsilon_{ij}\varepsilon_{ik} = \delta_{jk}$. When the static field is strong, i.e, for $\omega_B \tau \gg 1$, where $\omega_B = eE_0 L/\hbar$ is the Bloch frequency with L the lattice constant, σ_L and σ_H simplify to

$$\sigma_L(\omega, \mathbf{E}_0) = -\frac{e^2}{\hbar} \frac{\pi}{\tau \hbar V_c} \sum_{\mathbf{R}} \frac{R^2 \varepsilon_{-\mathbf{R}} f_{\mathbf{R}}^0}{\omega_{\mathbf{R}} (\omega - \omega_{\mathbf{R}} - \frac{i}{\tau})} = \frac{e^2}{\hbar} \frac{\pi}{V_c} \sum_{\mathbf{R}} \left(\frac{-R^2 \varepsilon_{-\mathbf{R}} f_{\mathbf{R}}^0}{\hbar \omega_{\mathbf{R}}} \right) \frac{(\omega - \omega_{\mathbf{R}}) \tau + i}{(\omega - \omega_{\mathbf{R}})^2 \tau^2 + 1}, \quad (\text{S39})$$

$$\sigma_H(\omega, \mathbf{E}_0) = \frac{e^2}{\hbar} \frac{\pi}{i\tau V_c} \sum_{\mathbf{R}} \frac{\Omega_{-\mathbf{R}} f_{\mathbf{R}}^0}{\omega - \omega_{\mathbf{R}} - \frac{i}{\tau}} = \frac{e^2}{\hbar} \frac{\pi}{V_c} \sum_{\mathbf{R}} (-i\Omega_{-\mathbf{R}} f_{\mathbf{R}}^0) \frac{(\omega - \omega_{\mathbf{R}}) \tau + i}{(\omega - \omega_{\mathbf{R}})^2 \tau^2 + 1}, \quad (\text{S40})$$

with $\omega_{\mathbf{R}} = e\mathbf{E}_0 \cdot \mathbf{R}/\hbar$.